A Coordinated Control Strategy for Multi-Feeder Clusters in Secondary Frequency Regulation Based on Direct OLTC Control

Fengming Shi, Siyang Liao*, Jian Xu, Deping Ke, Chong Han, Yujie Liang
School of Electrical and Automation
Wuhan University
Wuhan 430072, China
1951793307@qq.com

Lingfang Li
Yunnan Grid Research Construction and Planning Center of Yunnan Power Grid Co., Ltd.,
Kunming 650011, China
373621864@qq.com

***Abstract*—To address the demand for flexible regulation resources caused by the high penetration of renewable energy into the power grid, this paper proposes a secondary frequency regulation strategy for distribution network feeder clusters based on direct On-Load Tap Changer (OLTC) control, leveraging the untapped regulation potential of feeder loads. First, a Conservation Voltage Reduction (CVR) coefficient model is established based on the voltage-power coupling characteristics of feeder loads to characterize their regulation behavior. On this basis, with total system voltage security as a constraint, the dynamic regulation boundaries of the main transformer's low-voltage side bus voltage are solved. Combined with the identification results of the CVR coefficients, the real-time adjustable capacity of the feeder clusters is calculated to provide security constraints for dispatching agencies. Finally, a multi-objective regulation command decomposition optimization model is constructed, accounting for both user power quality and regulation accuracy. By adjusting OLTC tap positions, the coordinated response of multi-feeder clusters to secondary frequency regulation commands is achieved.**

***Index Terms*-- CVR coefficient, Voltage security, Adjustable capacity of feeder load, Coordination of multiple feeder clusters , Secondary frequency regulation**

I. INTRODUCTION

Confronted with pressures from the scarcity of traditional energy and mounting global carbon emissions, the world is advancing the energy transition and endeavoring to build a new power system featuring the synergy of "source-grid-load-storage" [1]. In this context, renewable energy sources like wind energy and photovoltaic energy have experienced rapid growth. Nevertheless, the randomness and fluctuating nature of their output have intensified the uncertainty on the source and load sides alike, which may trigger frequency deviations and system instability [2]. There is an imperative requirement to set up a new regulation system, so as to guarantee the safe, stable and cost-effective operation of the power grid.

Feeder load power control technology is based on the active power-voltage coupling characteristic of loads, achieving fast and precise control of load power through voltage regulation. This technology utilizes voltage regulation equipment [3-4] to directly control load power, effectively exploiting the regulation potential of the load side, thereby enhancing renewable energy integration capability and system stability. Given the limited regulation capacity of single nodes, this paper treats the feeder cluster connected to the same main transformer low-voltage bus as an integrated regulation unit [5], achieving direct power control through OLTC tap adjustment. Before participating in grid regulation, feeder loads need to report their regulation capability to support dispatch decisions. The assessment of adjustable capacity requires combining characteristic identification with voltage regulation boundary calculations. However, traditional methods focus only on the voltage at the point of common coupling [6], neglecting voltage differences among feeder nodes and the voltage safety constraints for end-users. Feeder clusters are directly controlled through grid-side equipment, eliminating the need for user negotiation and offering significant advantages in grid interaction. Existing research has incorporated feeder loads into regulation resource pools. Literature [7-8] proposes primary frequency regulation and automatic power control strategies based on direct feeder load control. Literature [9] explores coordinated multi-type voltage regulation to achieve energy conservation through voltage reduction for feeder loads. However, current research has not yet addressed feeder load participation in secondary frequency regulation for the grid, and the aforementioned methods do not consider the impact of the voltage regulation process on power quality at the user end.

To address these issues, this paper proposes a secondary frequency control strategy for feeder loads based on direct OLTC control. The main contributions are as follows: (1) A method for assessing the adjustable capacity of feeder clusters is proposed, which incorporates system-wide node voltage safety constraints and integrates the calculated low-voltage bus regulation boundaries of main transformers with feeder load characteristic identification, enabling precise evaluation

Funding: This research is supported by the National Key Research and Development Program of China (No.2023YFB2407300)
(*Corresponding author: Siyang Liao, liaosiyang@whu.edu.cn*)

979-8-3315-8138-1

of cluster regulation capability. (2) A secondary frequency control instruction decomposition model is constructed, balancing user power quality and regulation accuracy. By optimizing the OLTC tap adjustments of each main transformer, the precise response of multiple feeder clusters to frequency control instructions is achieved.

II. Modeling for Feeder Cluster Regulatory Traits and Assessment Method of Adjustable Capacity

A. Feeder Load Regulation Characteristic Model

Grid feeder loads consist of static and dynamic loads. Static loads are represented by the ZIP model, while dynamic loads (e.g., induction motors) are equivalent to constant impedance components when ignoring transients. Generally, loads with dominant constant impedance characteristics are more sensitive to voltage fluctuations, whereas constant power loads show weaker responses. The steady-state regulation characteristic is characterized by the Conservation Voltage Reduction (CVR) coefficient (Eq. 1), defined as the ratio of the percentage change in active power to the percentage change in voltage. This coefficient directly reflects the regulation capacity; a larger value indicates stronger potential.

$$f_{fcl}^{CVR} = \frac{\Delta P\%}{\Delta V\%} = \frac{\Delta P / P_0}{\Delta V / V_0} \tag{1}$$

Wherein, f_{fcl}^{CVR} stands for the CVR coefficient of the feeder cluster; ΔP and ΔV refer to the active power variation and voltage variation of the feeder cluster load, separately; P_0 and V_0 are the initial active power and initial voltage of the feeder of the identification cycle, respectively.

Grid operation measurement data of voltage and power are employed for parameter identification via the least squares method. By minimizing the sum of squared residuals between observed values and model-predicted values, to solve for the unknown parameters in the model, as shown in Equation (2).

$$f_{fcl}^{CVR} = \frac{\sum_{i=1}^{N_p} V_i^2 \sum_{i=1}^{N_p} P_i - \sum_{i=1}^{N_p} V_i \sum_{i=1}^{N_p} V_i P_i}{N_p \sum_{i=1}^{N_p} V_i^2 - \left(\sum_{i=1}^{N_p} V_i \right)^2} \tag{2}$$

V_i and P_i correspond to the measured values of feeder voltage and active power at the *i*-th sampling instant. N_P is the number of sampling points within the identification period. With feeder load composition changes, the CVR coefficient requires iterative updates to reflect its time-variation.

B. Evaluation for Adjustable Capacity of Feeder Clusters

In this paper, the feeder cluster connected to the same bus is regarded as a regulation unit, and the overall control of the active power of the feeder cluster is realized by changing the OLTC tap position. This section takes the voltage security of the distribution network as the core constraint, and based on power flow analysis, constructs an optimization model aiming to maximize the regulation range of the OLTC for the two operating scenarios of voltage increase and voltage decrease respectively. The formulations of the objective function are presented in Equations (3)-(4):

$$F_1 = \max\left(\Delta k_{up,t} \Delta V_{tap}\right) \tag{3}$$

$$F_2 = \max\left(\Delta k_{down,t} \Delta V_{tap}\right) \tag{4}$$

The OLTC is a discrete voltage regulation device, where ΔV_{tap} represents its unit voltage regulation step size, and $\Delta k_{up,t}$ and $\Delta k_{down,t}$ represent the OLTC's maximum adjustable upward and downward tap positions at instant t, respectively.

The following constraints must hold during optimization:

(1) Equality constraint of the basic power flow equation

$$P_{i,t}^{inj} = V_{i,t} \sum_{j=1}^{m} V_{j,t} \left(G_{ij} \cos\theta_{ij,t} + B_{ij} \sin\theta_{ij,t} \right) \tag{5}$$

$$Q_{i,t}^{inj} = V_{i,t} \sum_{j=1}^{m} V_{j,t} \left(B_{ij} \cos\theta_{ij,t} + G_{ij} \sin\theta_{ij,t} \right) \tag{6}$$

In this equation: *i* and *j* denote node numbers; $P_{i,t}^{inj}$ and $Q_{i,t}^{inj}$ correspond to the active and reactive power injected into node *i* at time *t*, respectively; $V_{i,t}$ and $V_{j,t}$ represent the voltage magnitudes at the line's beginning and end, respectively; G_{ij} and B_{ij} are the conductance and susceptance of the line, respectively; $\theta_{ij,t}$ refers to the voltage phase difference between the beginning and end of the line.

(2) Node Voltage Security Constraint

$$V_{\min} \le V_{i,t} \le V_{\max} \tag{7}$$

In the equation: $V_{i,t}$ is the actual voltage of node *i* at time *t*; $V_{\max}$ and $V_{\min}$ represent the upper and lower permissible voltage of node *i* in the distribution network, respectively;

(3) Operational Constraint of Voltage Regulation Equipment: Localized voltage optimization by utilizing user-side shunt reactive power control devices including distributed photovoltaics (PV) and static var compensators (SVC) can effectively enhance node voltage distribution, and is anticipated to extend the operational regulation boundary of the OLTC.

OLTC:

$$V_t^{\text{out}} = V_t^{\text{in}} + X_t^{\text{OLTC}} \Delta V_{\text{tap}} \tag{8}$$

$$X_{\min}^{\text{OLTC}} \le X_t^{\text{OLTC}} \le X_{\max}^{\text{OLTC}} \tag{9}$$

$$\left| X_t^{OLTC} - X_{t-1}^{OLTC} \right| \Delta t_{OLTC} \le T_C \tag{10}$$

$$\sum_{t \in T} \left| X_t^{\text{OLTC}} - X_{t-1}^{\text{OLTC}} \right| \le N_{\max}^{\text{OLTC}} \tag{11}$$

In this equation: V_t^{out} and V_t^{in} represent the pre-regulation and post-regulation voltages of the grid-connected point, respectively; X_t^{OLTC} is the tap position at time *t*; $X_{\max}^{\text{OLTC}}$ and $X_{\min}^{\text{OLTC}}$ are the upper and lower limits of the OLTC tap setting, respectively; Δt_{OLTC} denotes the single-step regulation duration of the OLTC, and T_C denotes the time interval for the dispatch center to issue control commands. $N_{\max}^{\text{OLTC}}$ is the allowable limit for the maximum count of tap changer switching times in a day.

PV:

$$P_{l,t}^{\text{PV}} = P_{l,t}^{\text{PVpre}} \tag{12}$$

$$\left|Q_{l,t}^{\text{PV}}\right| \le \sqrt{\left(S_l^{\text{PV}}\right)^2 - \left(P_{l,t}^{\text{PV}}\right)^2} \tag{13}$$

$$Q_l^{\text{PV,min}} \le Q_{l,t}^{\text{PV}} \le Q_l^{\text{PV,max}} \tag{14}$$

In this formula: $P_{l,t}^{\text{PV}}$ and $Q_{l,t}^{\text{PV}}$ denote the active output and reactive output of PV system l within time t; $Q_l^{\text{PV,max}}$ and $Q_l^{\text{PV,min}}$ represent the upper and lower bounds of the reactive power of PV system l; S_l^{PV} stands for the rated power capacity; $P_{l,t}^{\text{PVpre}}$ represents the predicted active power of PV system l during this time interval.

SVC:

$$Q_m^{\text{SVC,min}} \le Q_{m,t}^{\text{SVC}} \le Q_m^{\text{SVC,max}} \tag{15}$$

In the equation: $Q_{m,t}^{\text{SVC}}$ is the reactive power of the m-th SVC during the time period t; $Q_m^{\text{SVC,max}}$ and $Q_m^{\text{SVC,min}}$ represent the upper and lower reactive power limits of the SVC.

Capacitor Bank (CB):

$$Q_t^{CB} = X_t^{CB} Q^{CB\,R} \tag{16}$$

$$\sum_{t\in T}\left|X_t^{CB} - X_{t-1}^{CB}\right| \le N_{\max}^{CB} \tag{17}$$

Within the formula, $Q_t^{CB\,R}$ denotes the rated reactive capacity of the relevant switchable capacitor banks; X_t^{CB} represents the on-off state of the capacitor bank, where $X_t^{CB}=1$ the reactive power supplied by the capacitor in this state is $Q_t^{CB}=Q_t^{CB\,R}$. In contrast, when $X_t^{CB}=0$, the reactive power output is zero; $N_{\max}^{CB}$ denotes the maximum daily allowable limit for the capacitor bank's switching operations.

Under the prerequisite of upholding the voltage operation security of all system nodes, calculate the adjustable tap position boundary of OLTC. Based on this, determining the allowable voltage regulation range of the low-voltage side bus of the main transformer. Combined with the identification result of the CVR coefficient of the feeder cluster connected to this bus, precisely calculate the adjustable active power capacity scope of the feeder cluster.

$$\Delta P_{up,t}^{\text{Feeder}} = f_{fcl,t}^{CVR}\Delta k_{up,t}\Delta V_{tap} \tag{18}$$

$$\Delta P_{down,t}^{\text{Feeder}} = f_{fcl,t}^{CVR}\Delta k_{down,t}\Delta V_{tap} \tag{19}$$

In the equation, $f_{fcl,t}^{CVR}$ is the CVR coefficient of the feeder cluster; $\Delta P_{up,t}^{\text{Feeder}}$ and $\Delta P_{down,t}^{\text{Feeder}}$ represent the upward and downward adjustable load capacities of the feeder at moment t.

III. Coordinated Optimization Model for Secondary Frequency Modulation Based on Direct Control of Feeder Clusters

Since OLTCs operate discretely, feeder load clusters inevitably introduce power response deviations when complying with secondary frequency regulation commands. Furthermore, as the regulation behavior directly impacts user-side power quality, this paper proposes a multi-objective coordinated optimization model for feeder clusters that balances both regulation accuracy and power quality impact. The objective function is given in Equation 20.

$$\min J = \alpha_1\left|\Delta P_{AGC,t} - \sum_{i=1}^{N_{Cl}}\Delta P_{i,t}^{Feeder}\right| + \alpha_2\sum_{i=1}^{N_{Cl}}\sum_{j=1}^{N_{node,i}}\left|V_{ij,t}-V_N\right| \tag{20}$$

In the equation: $\Delta P_{AGC,t}$ represents the AGC(automatic generation control) command issued by the power grid to the feeder cluster during time period t. $\Delta P_{i,t}^{Feeder}$ is the active power regulation amount of the i-th feeder cluster; $V_{ij,t}$ is the voltage level of node j in the i-th feeder cluster; V_N is the rated voltage; $N_{node,i}$ is the number of nodes in the i-th feeder cluster; N_{Cl} is the number of feeder clusters participating in regulation; α_1 and α_2 are weight coefficients. The first term of the objective function aims to reduce the response deviation of grid commands and ensure the system frequency qualification rate, while the second term improves the power quality of electricity users by reducing the voltage deviation of each feeder load node.

The optimization procedure must adhere to the constraints listed below: (1) The equality constraints for the fundamental power flow equations, as specified in Section 2.B.

(2) Constraint on Adjustable Capacity of Feeder Loads:

$$\left|\Delta P_{up,t}\right| \le \Delta P_{up,t}^{\text{Feeder}} \tag{21}$$

$$\left|\Delta P_{down,t}\right| \le \Delta P_{down,t}^{\text{Feeder}} \tag{22}$$

where $\Delta P_{up,t}$ and $\Delta P_{down,t}$ denote the power upward and downward regulation instructions received by the feeder cluster during period t, respectively.

(3) Constraint on Grid Secondary Frequency Modulation Commands: Since the OLTC is a discrete regulation device, a certain degree of response deviation is allowed, which is represented by the maximum allowable deviation rate $R_{\max}^{\text{D}}$. The constraint is expressed as Equation 23:

$$\left|\frac{\Delta P_{AGC,t} - \Delta P_{total,t}^{Feeder}}{\Delta P_{AGC,t}}\right| \le R_{\max}^{D} \tag{23}$$

$\Delta P_{AGC,t}$ denotes the AGC command in time t, and $\Delta P_{total,t}^{Feeder}$ signifies the overall power response value of the feeder clusters during this duration.

IV. Case Study Analysis

A. Case Study Settings

Within this part, the IEEE 9-bus system serves as the main grid's fundamental structure. Meanwhile, direct-controlled distribution network load clusters connect to nodes 4, 5, and 8. Each cluster adopts the IEEE 33-bus topology, with the overall system structure shown in Figure 1:

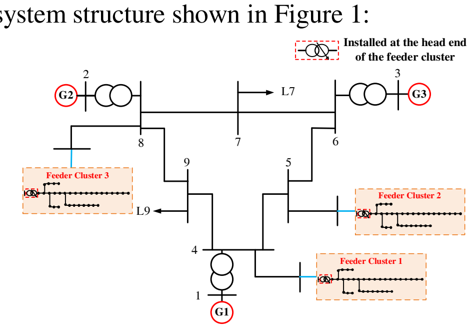

Figure 1. Improved IEEE 9-bus System Topology Structure

Each feeder cluster adopts a unified topology, with an 11-tap OLTC installed at the head end as the voltage regulation

979-8-3315-8138-1

device, and the regulation step is 0.0125 p.u. To meet frequency regulation requirements, the load base of the original IEEE 33-bus system is scaled up by 2, 2.5, and 3 times respectively, and the line admittances are reduced proportionally to ensure voltage security. The simulation duration is 15 minutes, with AGC commands issued every minute. In this case study, the feeders are equipped with ZIP load models, and the voltage-power coupling characteristics are simulated by modifying node power and connecting grounding impedances at each node. The identified CVR coefficients of the three feeder clusters are 1.856, 1.285, and 1.603.

B. Analysis of Regulation Effectiveness

A load disturbance is introduced at Node 7 to excite system dynamic responses, as shown in Fig. 2. Two scenarios are set for comparison: (1) feeder loads do not participate in frequency regulation; (2) the proposed control strategy is adopted to enable feeder loads to participate in secondary frequency regulation. Considering the impact of voltage regulation equipment response time on system frequency recovery, a first-order inertia link is used in Scenario 2 to simulate the delay of OLTC tap regulation, with time constants set to 5 s and 20 s for comparison. The comparison results of system frequency dynamic responses under the three cases are shown in Fig. 3.

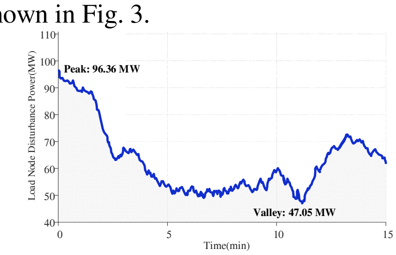

Figure 2. Active Power Disturbance Curve at Node 7

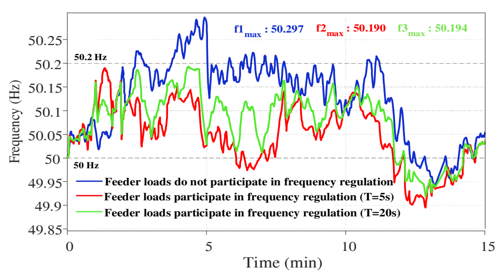

Figure 3. Pre- and Post-Regulation System Frequency Response Profiles with Feeder Load Participation

As shown in the figure 3, in Scenario 1, limited by thermal unit ramping constraints, the system lacks frequency regulation capacity. During load drop, output cannot be reduced quickly; frequency stays around 50.2 Hz long-term, peaking at 50.298 Hz with obvious over-limit. In contrast, integrating feeder clusters into the regulation pool greatly improves frequency regulation margin and optimizes system frequency, with both curves in Scenario 2 within the safe range. A comparison between the two cases with different response speeds shows that a smaller time constant leads to a faster regulation speed, a higher convergence rate of the system frequency to the nominal value (50 Hz), and a lower risk of frequency over-limit.

To systematically verify the effectiveness of the proposed control strategy, in the case study, under the same frequency regulation command, a strategy based on adjustable-capacity-proportional regulation task allocation is selected as the benchmark case, and a comparative analysis is carried out from two dimensions: response accuracy and impact on user power consumption. Figs. 4(a) and (b) show the tap adjustments of OLTC in the three feeder clusters under the two strategies in each period. Considering the regulation speed constraint of OLTCs in practical engineering, the case study specifies that the OLTC tap adjustment amount shall not exceed 3 steps in each control cycle. Fig. 5 compares the differences between the secondary frequency regulation command values and the power response values in each period. Fig. 6 presents the cumulative distribution of feeder node voltage deviations in each period.

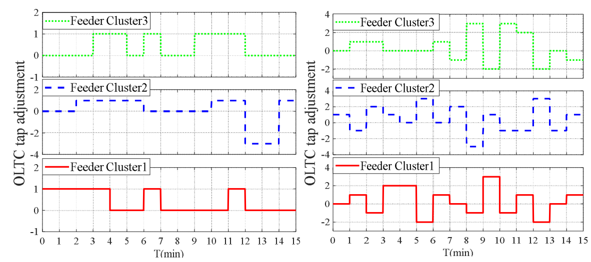

(a)Comparison Case (b)Proposed Method

Figure 4. OLTC Tap Position Status at Each Time Period

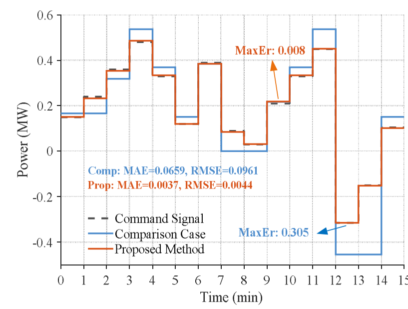

Figure 5. Comparison of Feeder Load Power Response under Two Regulation Strategies

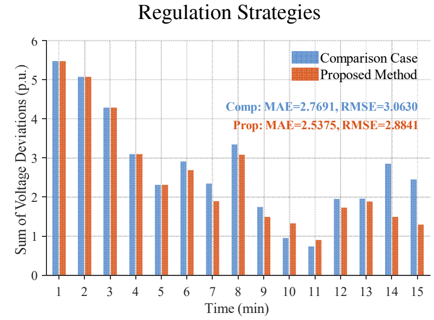

Figure 6. Comparison of Total Voltage Deviations at Nodes under Two Regulation Strategies

Based on the analysis of the power tracking curves shown in Figure 5, the optimization strategy proposed in this paper exhibits superior command tracking performance in each time period. Its response power values are closer to the AGC command curve compared with the comparative strategy of adjustable capacity allocation, ascertaining the improvement of the proposed method with respect to dynamic response accuracy. It should be noted that the OLTC tap position curves in Figure 4 reveal that due to the discrete regulation

979-8-3315-8138-1

characteristics of on-load tap changers, regulation errors are inevitably introduced. To compensate for this error, the power regulation direction of the three feeder clusters in the proposed strategy may temporarily reverse relative to the AGC command. In contrast, the traditional capacity allocation strategy adopts proportional allocation and does not induce such reverse regulation behavior. Further analysis regarding the voltage deviation statistics in Figure 6 shows that the sum of node voltage deviations of the proposed strategy is notably lower than that of the comparative scheme across most time periods, while deviation reversal occurs in some time periods. This is because the regulation action in each time period will change the network power flow distribution, thereby affecting the initial operating state of the next time period. If the comparison is based on the same initial state, the strategy proposed in this paper demonstrates better performance in suppressing voltage deviations.

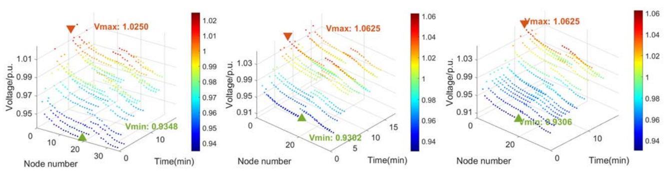

(a) Feeder Cluster 1 (b) Feeder Cluster 2 (c) Feeder Cluster 3

Figure 7. Voltage Conditions at Feeder Cluster Nodes During Response Intervals

As presented in the above figures, Figures 7(a)-(c) respectively illustrate the changes of voltage at each feeder node when the three feeder clusters respond to secondary frequency regulation commands. Analysis of the data in the figures reveals that under the regulation strategy proposed in this paper, all node voltages are stringently bounded within the safe operational range (0.93-1.07p.u.)[10] during the regulation process. This result indicates that the proposed method not only effectively tracks power grid dispatching commands but also accurately evaluates the adjustable capacity of feeder clusters, provides safety constraints for dispatching, ensures node voltage safety during regulation, and confirms the effectiveness and reliability of the proposed control strategy in sustaining the stable operation of the power grid.

V. CONCLUSION

This paper proposes a coordinated secondary frequency control method for multi-feeder clusters via direct OLTC control. For capacity assessment, the voltage regulation boundaries of the transformer's low-voltage bus and the available capacity of feeder clusters are determined based on system-wide node voltage security constraints, providing support for safe resource dispatch. Regarding optimal scheduling, a multi-objective instruction decomposition model is developed to balance response accuracy with consumer impact. Simulation results demonstrate that the strategy enables feeder clusters to accurately track frequency signals while suppressing voltage deviations and enhancing power quality.

However, frequent OLTC tap adjustments can accelerate mechanical wear and shorten equipment lifespan. Future research will focus on optimizing control terminal placement and developing instruction decomposition algorithms aimed at reducing switching frequency to extend equipment life. Furthermore, the integration of advanced voltage regulation devices, such as smart transformers, DVRs, and renewable energy inverters, will be explored to enhance the flexibility of feeder load participation in grid-load interaction.

REFERENCES

[1] W. Li, J. Wang, E. Du, P. Wang, N. Zhang, and C. Kang, “Planning Coal Power Generation Transition Considering Multiple Alternatives With a Full Life Cycle Perspective,” *IEEE Trans. Power Syst*., vol. 40, no. 6, pp. 5171–5183, Nov. 2025.

[2] M. Yang, T. Wang, X. Zhang, W. Zhang, and B. Wang, “Considering Dynamic Perception of Fluctuation Trends for Long-Foresight-Term Wind Power Prediction,” *Energy*, vol. 289, Art. no. 130016, Feb. 2024.

[3] S. Hayward, M. Merlin, M. Williams, and T. Morstyn, “Coordination of Smart Hybrid Transformers in Distribution Networks,” *IEEE Trans. Smart Grid*, vol. 16, no. 2, pp. 973–988, Mar. 2025.

[4] Q. Zhang, Y. Guo, Z. Wang, and F. Bu, “Distributed optimal conservation voltage reduction in integrated primary-secondary distribution systems,” *IEEE Trans. Smart Grid*, vol. 12, no. 5, pp. 3889–3900, Sep. 2021.

[5] S. Liao, F. Shi, J. Xu, D. Ke, Y. Sun, and H. Zhang, “Dynamic Assessment Method for Virtual Power Plant Regulation Capability Based on Direct Control of Feeder Load Clusters,” *Autom. Electr. Power Syst*., vol. 49, no. 20, pp. 73–83, Oct. 2025.

[6] H. Sun, X. Ding, Z. Wu, S. Zheng, and Z. Xu, “Voltage Regulation Strategy for Distribution Network Considering Optimal Adjustment of Automatic Voltage Control System Limits,” *Autom. Electr. Power Syst*., vol. 49, no. 12, pp. 184–193, Jun. 2025.

[7] Q. Zhang, Y. Guo, Z. Wang, and F. Bu, “Distributed Optimal Conservation Voltage Reduction in Integrated Primary-Secondary Distribution Systems,” *IEEE Trans. Smart Grid*, vol. 12, no. 5, pp. 3889–3900, Sep. 2021.

[8] J. Xu, X. Lei, S. Liao, D. Ke, and Y. Sun, “Automatic Power Control of Direct-controlled Virtual Power Plant Based on Multi-feeder Load Coordination in Distribution Network,” *Autom. Electr. Power Syst*., vol. 48, no. 24, pp. 22–32, Dec. 2024.

[9] F. Ding and M. Baggu, “Coordinated Use of Smart Inverters With Legacy Voltage Regulating Devices in Distribution Systems With High Distributed PV Penetration—Increase CVR Energy Savings,” *IEEE Trans. Smart Grid*, vol. 14, no. 3, pp. 1804–1813, May 2023.

[10] China National Standard GB/T 12325-2008. "Power Quality – Deviation of Supply Voltage" [S]. 2008.

979-8-3315-8138-1